

## Measurements of Energy Correlations in $e^+e^- \rightarrow$ Hadrons

JADE Collaboration

W. Bartel, L. Becker, C. Bowdery<sup>1</sup>, D. Cords<sup>2</sup>, R. Felst, D. Haidt, H. Junge<sup>3</sup>, G. Knies, H. Krehbiel, P. Laurikainen<sup>4</sup>, R. Meinke, K. Meissner, B. Naroska, J. Olsson, E. Pietarinen<sup>4</sup>, D. Schmidt<sup>3</sup>, P. Steffen, P. Warming, M. Zachara

Deutsches Elektronen-Synchrotron DESY, D-2000 Hamburg, Federal Republic of Germany

G. Dietrich, E. Elsen<sup>2</sup>, G. Heinzelmann, H. Kado, M. Kuhlen, T. Mashimo, K. Meier, A. Petersen, U. Schneekloth, G. Weber

II. Institut für Experimentalphysik der Universität, D-2000 Hamburg, Federal Republic of Germany

K. Ambrus, S. Bethke, A. Dieckmann, J. Heintze, K.H. Hellenbrand, R.D. Heuer<sup>5</sup>, S. Komaniya, J. von Krogh, P. Lennert, H. Matsumura, H. Rieseberg, J. Spitzer, A. Wagner

Physikalisches Institut der Universität, D-6900 Heidelberg, Federal Republic of Germany

A. Finch, F. Foster, G. Hughes, T. Nozaki, J. Nye

University, Lancaster LA1 4YB, England

J. Allison, J. Baines, A.H. Ball, R.J. Barlow, J. Chrin, I.P. Duerdoth, T. Greenshaw, P. Hill, F.K. Loebinger, A.A. Macbeth, H. McCann, H.E. Mills, P.G. Murphy, K. Stephens

University, Manchester M13 9PL, England

R.G. Glasser, B. Sechi-Zorn, J.A.J. Skard, S. Wagner, G.T. Zorn

University of Maryland, MD20742, USA

S.L. Cartwright, D. Clarke, R. Marshall, J.B. Whittaker

Rutherford Appleton Laboratory, Chilton, Didcot, Oxon OX11 0QX, England

J. Kanzaki, T. Kawamoto, T. Kobayashi, M. Koshihara, M. Minowa, M. Nozaki, S. Orito, A. Sato, H. Takeda, T. Takeshita, Y. Totsuka, S. Yamada

Lab. of Int. Coll. on Elementary Particle Physics and Department of Physics, University of Tokyo, Japan

Received 19 June 1984

**Abstract.** Energy-energy-correlations (EEC) have been measured with the JADE detector at c.m. energies of 14 GeV, 22 GeV and in the region  $29 \text{ GeV} < E_{\text{cm}} < 36 \text{ GeV}$ . Corrected results are pre-

sented of EEC and their asymmetry, which can be directly compared to theoretical predictions. At  $\langle E_{\text{cm}} \rangle = 34 \text{ GeV}$  a comparison with second order QCD predictions yields good agreement for the string model fragmentation resulting in a value of the strong coupling constant  $\alpha_s = 0.165 \pm 0.01$  (stat.)  $\pm 0.01$  (syst.). The independent fragmentation models, which yield values of  $\alpha_s$  between 0.10 and 0.15 depending on the treatment of energy and momentum conservation and of the gluon splitting, do not pro-

<sup>1</sup> European Science Exchange Fellow

<sup>2</sup> Now at SLAC, California, USA

<sup>3</sup> Universität-Gesamthochschule Wuppertal, Germany

<sup>4</sup> University Helsinki, Helsinki, Finland

<sup>5</sup> Now at CERN, Geneva, Switzerland

vide a satisfactory description of the data over the full angular range.

## Introduction

Energy-energy-correlations (EEC) between particles produced by  $e^+e^-$  annihilation at high energies have been extensively studied theoretically in the framework of perturbative QCD. EEC were proposed by Dokshitzer et al. [1] and by Basham et al. [2], who studied them in the first order of strong coupling strength  $\alpha_s$  and showed that they are calculable in perturbative QCD. Recently EEC have been calculated in order  $\alpha_s^2$  by Ali et al. [3] and by Richards et al. [4]. It has been claimed [5] that especially the asymmetry of the EEC is little dependent on the fragmentation of quarks and gluons into hadrons, and that this therefore should allow an accurate determination of the strong coupling constant  $\alpha_s$ .

In this paper we present energy-energy-correlations measured with the JADE detector at PETRA. The data are corrected for the effects of the detector acceptance and resolution as well as for the effects of photon-bremsstrahlung, and can be compared with theoretical calculations. We also study how different fragmentation schemes affect the theoretical predictions and estimate the uncertainties they cause for the determination of  $\alpha_s$ . Finally we show, that the fragmentation model of the Lund group yields a better description of the EEC than models with independent parton fragmentation.

The first analysis of EEC was performed by the PLUTO [6] group, followed by results from the Mark II [7], CELLO [8], and Mark J [9] groups. The Mark J groups finds that a comparison of the data with second order QCD prediction is nearly independent of the fragmentation model while the CELLO analysis yields a considerable model dependence both in first and second order.

For the definition of the EEC consider two particles  $i$  and  $j$  produced in the reaction

$$e^+e^- \rightarrow i+j+X. \quad (1)$$

The normalized energies are  $x_i = E_i/E_{\text{cm}}$  and  $\theta$  is the angle between particles  $i$  and  $j$ . The energy weighted normalized two-particle differential cross section is then

$$\frac{d\Sigma}{d\theta} = \frac{1}{\sigma_{\text{tot}}} \sum_{i,j} \int dx_i dx_j x_i x_j \frac{d^3\sigma}{dx_i dx_j d\theta} \quad (2)$$

where  $i, j$  run over all hadrons produced in reaction (1), i.e. all particle combinations including  $i=j$  con-

tribute to the sum and the normalization is by definition

$$\int \frac{d\Sigma}{d\theta} d\theta = 1. \quad (3)$$

For 2-jet events  $d\Sigma/d\theta$  is expected to be symmetric around  $90^\circ$ . Neglecting transverse momenta a 2-jet event would contribute with equal strength at  $\theta=0^\circ$  and  $\theta=180^\circ$  only, and finite transverse momenta are expected to smear these contributions. For 3-jet events  $d\Sigma/d\theta$  is in general no longer symmetric around  $90^\circ$ . For instance, a threefold symmetric event, neglecting the momentum components transverse to the jet direction, contributes at  $\theta=0^\circ$  and  $120^\circ$  only. The asymmetry

$$A(\theta) = \frac{d\Sigma(\pi-\theta)}{d\theta} - \frac{d\Sigma(\theta)}{d\theta} \quad (4)$$

is therefore expected to be especially sensitive to the effects of gluon emission.

## Data

The data have been taken with the JADE detector at PETRA at c.m. energies of 14 GeV, 22 GeV and in the region  $29 \text{ GeV} < E_{\text{cm}} < 36 \text{ GeV}$  with  $\langle E_{\text{cm}} \rangle = 34 \text{ GeV}$ . A detailed description of the detector, the trigger conditions and the selection of hadronic events is given in [10]. Both charged and neutral particles with momenta exceeding 100 MeV/c and 150 MeV/c respectively are used in the analysis.

The following cuts were applied in addition to those mentioned in [10].

$$(I) |\cos \theta_{\text{sph}}| < 0.9$$

$\theta_{\text{sph}}$  = angle between the sphericity axis and the  $z$ -axis which is in the beam direction.

$$(II) |\mathbf{p}_{\text{mis}}| < \frac{1}{4} E_{\text{cm}}$$

$\mathbf{p}_{\text{mis}}$  = missing momentum.

$$(III) |p_{z\text{mis}}|/|\mathbf{p}_{\text{mis}}| < 0.85 \text{ for } |\mathbf{p}_{\text{mis}}| > 2 \text{ GeV}/c$$

$p_{z\text{mis}}$  =  $z$  component of  $\mathbf{p}_{\text{mis}}$ .

(IV) An isolated neutral particle was searched for by the cluster method described in [11]. An event was rejected if this method yielded a cluster containing only one neutral particle of energy  $E > 3 \text{ GeV}$ .

The cuts (III) and (IV) were applied to eliminate those events with hard bremsstrahlung photons, since in this case two-jet events also cause an asymmetry  $A(\theta)$ . After these cuts, the data samples consist of 2,112 events at  $E_{\text{cm}} = 14 \text{ GeV}$ , 1,399 events at  $E_{\text{cm}} = 22 \text{ GeV}$  and 12,719 events at  $E_{\text{cm}} = 34 \text{ GeV}$ .

The quantity  $d\Sigma/d\theta$  is computed from the raw data by the following procedure:

$$[d\Sigma/d\theta]_{\text{exp}}^{\text{uncor}} = \frac{1}{N} \sum_k \sum_{i,j} x_i^k x_j^k \frac{1}{\Delta\theta} \int_{\theta-\Delta\theta/2}^{\theta+\Delta\theta/2} \delta(\theta_{i,j}^k - \theta') d\theta'$$

where the index  $k$  extends over all events in the data sample and the summation over  $i, j$  extends over all particle pairings of an individual event.  $\Delta\theta$  is the bin width in  $\theta$ , chosen to be  $3.6^\circ$ , and  $x_i = E_i/E_{\text{vis}}$ , where  $E_{\text{vis}}$  is the energy sum of all particles observed in an event. This procedure does not require the determination of jet axes.

The resulting distribution is corrected for detection efficiencies, resolution effects and for the effects of photon bremsstrahlung of the initial state leptons. The corrections, which are determined by Monte Carlo techniques, are applied bin by bin and are given by the ratio of the model results with (realist.) and without (ideal) the inclusion of these effects:

$$\left[\frac{d\Sigma}{d\theta}\right]_{\text{exp}} = \left[\frac{d\Sigma}{d\theta}\right]_{\text{exp}}^{\text{uncor.}} \cdot \left[\frac{d\Sigma}{d\theta}\right]_{\text{MC}}^{\text{ideal}} / \left[\frac{d\Sigma}{d\theta}\right]_{\text{MC}}^{\text{realist.}}$$

The correction factors applied at the various  $\theta$  bins and cm energies, which have been obtained using the Lund model [12], are shown in Fig. 1. It has been verified that these correction factors remain within the errors shown, if instead of the Lund model the fragmentation scheme of Hoyer et al. [13] or Ali et al. [14] is used.

The same correction procedure is applied to the asymmetry  $A(\theta)$

$$A(\theta)_{\text{exp}} = A(\theta)_{\text{exp}}^{\text{uncor.}} \cdot A(\theta)_{\text{MC}}^{\text{ideal}} / A(\theta)_{\text{MC}}^{\text{realist.}}$$

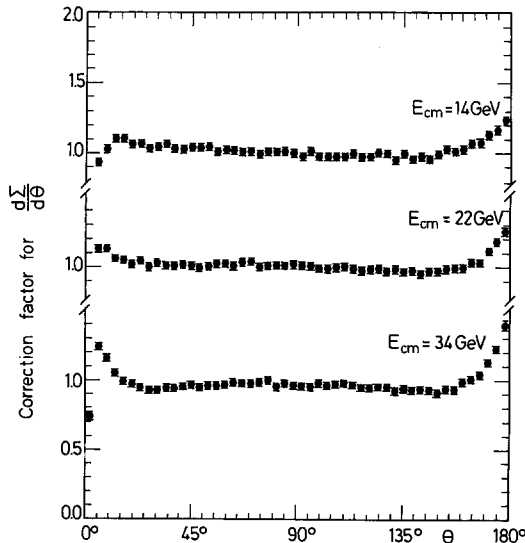


Fig. 1. The correction factor for  $d\Sigma/d\theta$  at three c.m. energies calculated by the Lund model

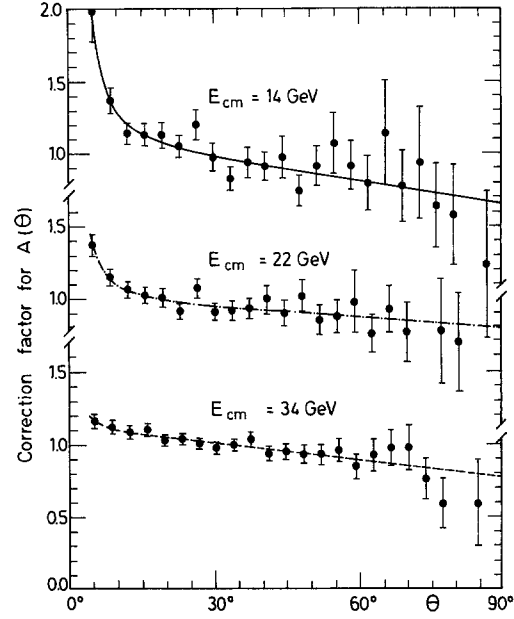


Fig. 2. The correction factor for the asymmetry  $A(\theta)$  calculated by the Lund model. The curves interpolate the points and were used to correct the data

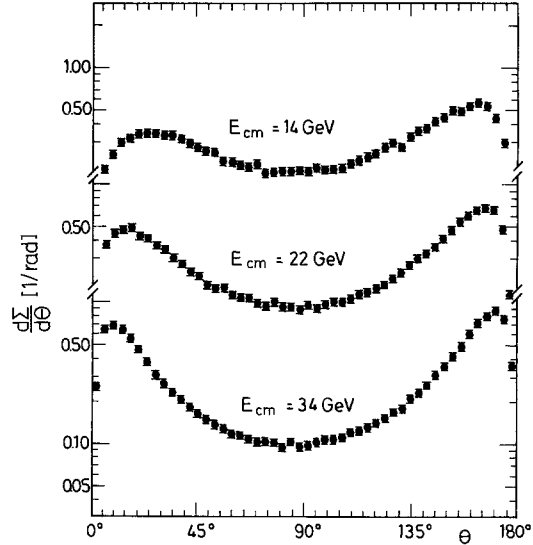


Fig. 3. The corrected  $d\Sigma/d\theta$  data at  $E_{\text{cm}} = 14, 22$  and  $34$  GeV

In comparison to the standard procedure in which  $A(\theta)_{\text{exp}}$  is directly determined from  $[d\Sigma/d\theta]_{\text{exp}}$ , this has the advantage that corrections symmetric in  $\theta$  cancel out. The correction factors for  $A(\theta)$ , obtained with the Lund model, are shown in Fig. 2. Using the other models instead of the Lund model does not change these correction factors for  $\theta > 20^\circ$ .

Comparing, for instance, the data corrected by different model results with QCD predictions for

$\theta > 40^\circ$  yields the same values of  $\alpha_s$  within 0.01. For  $\theta < 15^\circ$  the corrected  $A(\theta)_{\text{exp}}$  show differences of about 10–15% depending on whether the corrections were determined with the Lund model or the models based on independent parton fragmentation. To reduce the effect of statistical fluctuations, the bin

**Table 1.** Numerical values of  $d\Sigma/d\theta_{\text{exp}}$  as explained in the text

$\theta$ (degree)	$d\Sigma/d\theta * 10^3$ (1/rad)		
	$E_{\text{cm}} = 14$ GeV	$E_{\text{cm}} = 22$ GeV	$E_{\text{cm}} = 34$ GeV
0.0– 3.6	1,530 ± 40	1,670 ± 40	1,805 ± 40
3.6– 7.2	193 ± 8	370 ± 20	634 ± 15
7.2– 10.8	245 ± 10	445 ± 19	685 ± 15
10.8– 14.4	299 ± 11	472 ± 16	637 ± 13
14.4– 18.0	319 ± 11	490 ± 16	556 ± 12
18.0– 21.6	341 ± 11	430 ± 15	466 ± 10
21.6– 25.2	348 ± 11	414 ± 15	381 ± 8
25.2– 28.8	347 ± 11	369 ± 13	311 ± 7
28.8– 32.4	337 ± 10	346 ± 13	271 ± 6
32.4– 36.0	333 ± 10	301 ± 12	235 ± 6
36.0– 39.6	316 ± 10	273 ± 11	208 ± 5
39.6– 43.2	293 ± 9	242 ± 11	185 ± 5
43.2– 46.8	273 ± 9	225 ± 11	166 ± 4
46.8– 50.4	257 ± 9	195 ± 11	150 ± 4
50.4– 54.0	253 ± 9	185 ± 11	137 ± 4
54.0– 57.6	221 ± 9	186 ± 11	128 ± 4
57.6– 61.2	216 ± 9	164 ± 11	118 ± 4
61.2– 64.8	207 ± 9	158 ± 11	115 ± 4
64.8– 68.4	200 ± 9	157 ± 11	109 ± 4
68.4– 72.0	210 ± 9	144 ± 11	104 ± 4
72.0– 75.6	183 ± 9	137 ± 11	104 ± 4
75.6– 79.2	184 ± 9	149 ± 11	102 ± 4
79.2– 82.8	187 ± 9	137 ± 11	99 ± 4
82.8– 86.4	188 ± 9	136 ± 11	104 ± 4
86.4– 90.0	191 ± 9	131 ± 11	99 ± 4
90.0– 93.6	187 ± 9	140 ± 11	103 ± 4
93.6– 97.2	200 ± 9	134 ± 11	104 ± 4
97.2– 100.8	193 ± 9	142 ± 11	108 ± 4
100.8– 104.4	194 ± 9	150 ± 11	108 ± 4
104.4– 108.0	198 ± 9	148 ± 11	112 ± 4
108.0– 111.6	213 ± 9	157 ± 11	121 ± 4
111.6– 115.2	225 ± 9	168 ± 11	125 ± 5
115.2– 118.8	238 ± 9	174 ± 11	133 ± 5
118.8– 122.4	251 ± 9	184 ± 11	143 ± 5
122.4– 126.0	278 ± 9	196 ± 11	155 ± 5
126.0– 129.6	299 ± 9	215 ± 11	171 ± 5
129.6– 133.2	280 ± 9	238 ± 11	182 ± 5
133.2– 136.8	332 ± 10	269 ± 11	214 ± 6
136.8– 140.4	359 ± 11	301 ± 11	235 ± 8
140.4– 144.0	380 ± 11	323 ± 13	265 ± 9
144.0– 147.6	421 ± 12	363 ± 14	311 ± 10
147.6– 151.2	448 ± 13	419 ± 15	356 ± 10
151.2– 154.8	506 ± 15	474 ± 16	419 ± 10
154.8– 158.4	500 ± 15	549 ± 18	493 ± 14
158.4– 162.0	545 ± 17	597 ± 19	604 ± 14
162.0– 165.6	576 ± 19	653 ± 20	720 ± 17
165.6– 169.2	541 ± 20	682 ± 25	807 ± 20
169.2– 172.8	448 ± 20	667 ± 28	881 ± 20
172.8– 176.4	301 ± 20	486 ± 25	755 ± 20
176.4– 180.0	120 ± 14	167 ± 20	341 ± 20

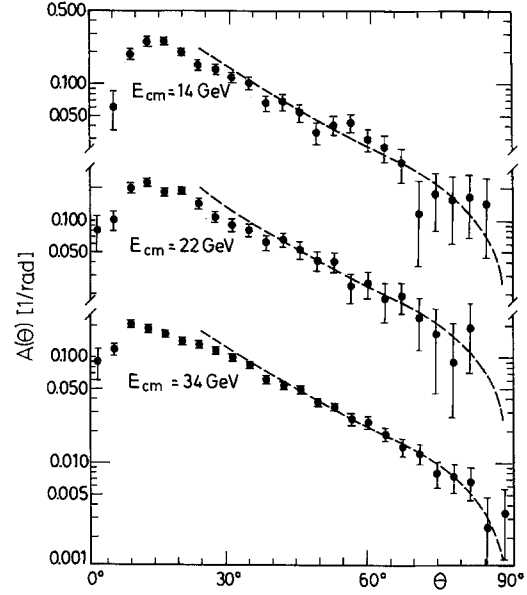


**Fig. 4.** The corrected asymmetries  $A(\theta)$  at  $E_{\text{cm}} = 14, 22$  and  $34$  GeV. The lines represent fits using the  $O(\alpha_s)^2$  calculation given in [3] not including fragmentation effects. The resulting values are  $\alpha_s = 0.14 \pm 0.01$ ,  $\alpha_s = 0.13 \pm 0.01$ ,  $\alpha_s = 0.115 \pm 0.005$  at  $E_{\text{cm}} = 14, 22$  and  $34$  GeV respectively. The errors contain only the uncertainty from the fit.

**Table 2.** Numerical values of  $A(\theta)_{\text{exp}}$  as explained in the text

$\theta$ (degree)	$A(\theta) * 10^3$ (1/rad)		
	$E_{\text{cm}} = 14$ GeV	$E_{\text{cm}} = 22$ GeV	$E_{\text{cm}} = 34$ GeV
0.0– 3.6	−1,420 ± 40	−1,460 ± 40	−1,500 ± 40
3.6– 7.2	61 ± 24	101 ± 21	118 ± 15
7.2– 10.8	190 ± 20	204 ± 20	206 ± 15
10.8– 14.4	253 ± 20	231 ± 20	186 ± 15
10.4– 18.0	257 ± 18	186 ± 17	165 ± 10
18.0– 21.6	200 ± 16	191 ± 15	140 ± 10
21.6– 25.2	152 ± 15	145 ± 14	128 ± 7
25.2– 28.8	138 ± 13	107 ± 12	112 ± 6
28.8– 32.4	115 ± 12	89 ± 11	97 ± 6
32.4– 36.0	102 ± 12	80 ± 10	81 ± 5
36.0– 39.6	66 ± 10	61 ± 10	59 ± 4
39.6– 43.2	69 ± 10	65 ± 9	51 ± 4
43.2– 46.8	54 ± 9	52 ± 9	47 ± 4
46.8– 50.4	35 ± 8	41 ± 8	36 ± 3
50.4– 54.0	41 ± 8	40 ± 8	32 ± 3
54.0– 57.6	43 ± 8	24 ± 7	25 ± 3
57.6– 61.2	30 ± 7	25 ± 7	23 ± 3
61.2– 64.8	25 ± 7	18 ± 7	17 ± 2
64.8– 68.4	18 ± 6	19 ± 6	13 ± 2
68.4– 72.0	6 ± 6	12 ± 6	11 ± 2
72.0– 75.6	9 ± 5	8 ± 6	7 ± 2
75.6– 79.2	8 ± 5	4 ± 6	7 ± 2
79.2– 82.8	8 ± 5	9 ± 6	6 ± 2
82.8– 86.4	7 ± 5	1 ± 5	2 ± 2
86.4– 90.0	0 ± 5	1 ± 5	3 ± 2

correction factors shown in Fig. 2 were interpolated by the curves shown, and these interpolated values were used to correct the data. It should be pointed out that without the cuts (III) and (IV) the corrections turn out to be considerably larger and model dependent because also photon bremsstrahlung effects yield an asymmetry.

The corrected data are shown in Fig. 3 for  $d\Sigma/d\theta$  and in Fig. 4 for  $A(\theta)$  and in tabulated form in

Table 1 and 2, respectively. Whereas the tables contain the selfcorrelation ( $i=j$ ), it is taken off in the figures.

### Comparison with QCD Models

The model calculations are based on a computer code written by Sjöstrand [15], which generates

**Tables 3a and 3b.** Comparisons of QCD predictions with data for several fragmentation parameters. The first number of each column represents the  $\alpha_s$  value obtained from the fit to the asymmetry of the region  $\theta > 36^\circ$ , the second one the  $\alpha_s$  value from the fit to the EEC in the region  $54^\circ < \theta < 126^\circ$ , and the third one the  $\chi^2$  value of this fit to the EEC summed over the full  $\theta$ -range. In **a** these numbers are given for  $A=1.0$  and various values of  $\sigma_q$  and  $B$ ; in **b** for  $\sigma_q=280$  MeV and various values of  $A$  and  $B$ . A value of  $y_{\min}=0.02$  was used in all cases

$\sigma_q$	$B$	$\alpha_s$ values and $\chi^2$								
		0.2	0.4	0.55	0.7	0.85	1.00	1.15	1.3	
350 MeV		$\alpha_s(A(\theta))$		0.169						
		$\alpha_s(d\Sigma/d\theta)$		0.151						
		$\chi^2(d\Sigma/d\theta)$		167						
315 MeV		0.183		0.169	0.163	0.155			0.155	
		0.113		0.151	0.159	0.169			0.181	
		197		108	151	199			317	
280 MeV		0.191	0.181	0.168	0.165	0.157				
		0.123	0.143	0.159	0.168	0.172				
		143	98	99	141	215				
245 MeV		0.191	0.172	0.169	0.157	0.156			0.153	
		0.129	0.149	0.161	0.169	0.177			0.187	
		112	93	96	171	260			433	
210 MeV		0.175		0.163		0.155				
		0.137		0.169		0.183				
		87		244		307				

$A$	$B$	$\alpha_s$ values and $\chi^2$							
		0.2	0.4	0.55	0.7	0.85	1.00	1.15	1.3
1.3				0.175	0.171				
				0.140	0.155				
				85	103				
1.0		0.203	0.191	0.181	0.168	0.165	0.157		
		0.080	0.123	0.143	0.159	0.168	0.172		
		411	143	98	99	141	215		
0.7		0.175		0.168	0.170	0.150			
		0.143		0.159	0.170	0.177			
		87		113	153	243			
0.5		0.183	0.165	0.157					
		0.113	0.153	0.165					
		159	123	193					
0.2		0.168	0.155	0.147					
		0.141	0.170	0.183					
		122	257	406					
0.1		0.157							
		0.149							
		162							

quarks and gluons according to the distributions of perturbative QCD including  $\alpha_s^2$  effects [16]. The invariant masses  $m_{ij}$  between partons  $i$  and  $j$  are used to distinguish different parton classes. If  $y = m_{ij}/s < y_{\min}$ , then the four-momenta of the partons  $i$  and  $j$  are combined.

The connection between partons and hadrons proceeds via a Field and Feynman like iterative cascade jet model. The various models, which can be chosen by the program, differ in the fragmentation axes, the way energy momentum conservation is enforced and in the treatment of the gluon fragmentation. The following schemes were used:

1) The string fragmentation of the Lund group, where the fragmentation occurs along the colour strings which are stretched from the quark via gluon(s) to the antiquark [12].

2) Independent fragmentation of the partons along their momentum direction in the overall c.m.s. The method of momentum conservation according to Hoyer et al. [13] is to conserve transverse momentum locally within each jet and then to rescale longitudinal momenta separately for each jet such that the ratio of jet over parton momentum is the same for  $q, \bar{q}$  and  $g$ . The ratio is chosen such that the correct total energy is also obtained.

3) As (2), but enforcing energy-momentum conservation according to Ali et al. [14] by boosting first all hadrons such that the momentum is conserved and thereafter rescaling the momenta to conserve the energy.

While the gluon fragmentation is essentially fixed in the string model, different treatments of the gluon are possible in the schemes (2) and (3). We have studied the following cases:

a) The gluon is treated as a  $q\bar{q}$ -pair, where the momentum in the overall cms is carried by one of the quarks only ( $g=q$ ).

b) The gluon momentum is shared between quark and antiquark according to the Altarelli-Parisi function [17].

c) The gluon momentum is equally shared between quark and antiquark.

For all models the fragmentation proceeds essentially according to the Field Feynman scheme, i.e. a Gaussian  $p_{\perp}$  distribution of the secondary quarks with a variance of  $\sigma_q^2$  and a longitudinal fragmentation function [18]

$$f(z) = (1-z)^A e^{(-Bm_{\perp}^2/z)}$$

where  $m_{\perp}$  is the transverse mass of the produced hadron and  $A$  and  $B$  are free parameters. Equal fractions of pseudoscalar and vector mesons and a production ratio of secondary  $u, d$  and  $s$  quark pairs

of 3:3:1 are assumed. In case of string fragmentation, the reader can estimate the parameter dependence of the model predictions on  $d\Sigma/d\theta$  and  $A(\theta)$  from Table 3. There are three numbers given for different values of the parameter pairs  $(\sigma_q, B)$  in Table 3a and  $(A, B)$  in Table 3b. The first of these numbers is the  $\alpha_s$  value obtained by fitting to the data on  $A(\theta)$  for  $\theta \geq 36^\circ$ , the second number is the  $\alpha_s$  value obtained from a fit to the data on  $d\Sigma/d\theta$  in the region  $54^\circ < \theta < 126^\circ$ , and the third number represents the  $\chi^2$  of this fit to  $d\Sigma/d\theta$  for the full range of  $\theta$ . The Lund model has been used with  $y_{\min} = 0.02$  and  $A = 1$  for Table 3a and  $\sigma_q = 280$  MeV for Table 3b. The  $\alpha_s$ , determined from  $A(\theta)$  depends only weakly on  $\sigma_q$  and somewhat stronger on the fragmentation parameters  $A$  and  $B$ . For all given sets of parameters the asymmetry for  $\theta > 36^\circ$  can be well described with  $\chi^2/\text{d.f.} < 1$ , but the region  $\theta < 30^\circ$  is by no parameter set well reproduced as long as  $y_{\min} \geq 0.02$ .

The data on  $A(\theta)$  for  $\theta < 30^\circ$  could only be fully reproduced by the Lund model for  $y_{\min} < 0.02$ . For these values of  $y_{\min}$ , effects of the order  $\alpha_s^3$  are probably not negligible. Taking  $y_{\min} = 0.0125$  and  $\alpha_s = 0.165$  3-parton and 4-parton events essentially saturate the total cross section:  $\sim 5\%$  2-parton,  $\sim 80\%$  3-parton and  $\sim 15\%$  4-parton events. Fig. 5 shows the dependence of the model results on  $y_{\min}$ , where, for better comparison, both  $d\Sigma/d\theta$  and  $A(\theta)$

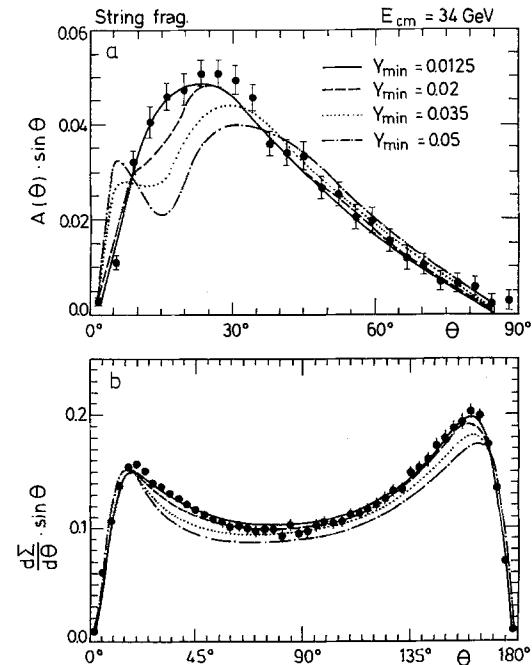


**Fig. 5a and b.** Comparison of the asymmetry  $A(\theta)$  **a** and the EEC  $d\Sigma/d\theta$  **b** at  $E_{\text{cm}} = 34$  GeV with the QCD results using the string model fragmentation for different  $y_{\min}$  values. The following parameters are used:  $\alpha_s = 0.165$ ,  $\sigma_q = 265$  MeV,  $A = 1.0$  and  $B = 0.75$

are multiplied by  $\sin\theta$ . It is seen that the small angle region of  $A(\theta)$ , which is usually described by the fragmentation is quite sensitive to soft and collinear gluon emission. The region  $40^\circ < \theta < 70^\circ$  of  $A(\theta)$  is only slightly affected by the  $y_{\min}$  cut.

Summarizing this comparison, we note, that the strong coupling strength deduced at  $\sqrt{s} = 34 \text{ GeV}$  using the string fragmentation scheme is  $\alpha_s = 0.165 \pm 0.01$ , which for  $y_{\min} = 0.0125$  and the best fit parameters  $\sigma_q = 220 \text{ MeV}$ ,  $A = 1.0$  and  $B = 0.70 \text{ GeV}^{-2}$  describes both the  $A(\theta)$  and  $d\Sigma/d\theta$  data well (see Fig. 6). These parameters also provide within the Lund model a good description of many other particle distributions.

A similar comparison, using the independent fragmentation schemes instead of the string model, yields lower values of  $\alpha_s$  from the asymmetry. Within these models and considering only the region  $\theta > 36^\circ$ ,  $A(\theta)$  is found to be nearly independent of the parameters  $A, B$  and  $\sigma_q$ . This is demonstrated in Figs. 7a and 8a, where the model predictions are plotted for the scheme (2) (c) with  $\alpha_s = 0.105$ ,  $Y_{\min} = 0.0125$  and various values of  $A, B$  and  $\sigma_q$ .

We did not succeed, however, in reproducing  $A(\theta)$  for  $\theta < 30^\circ$  with the independent fragmentation

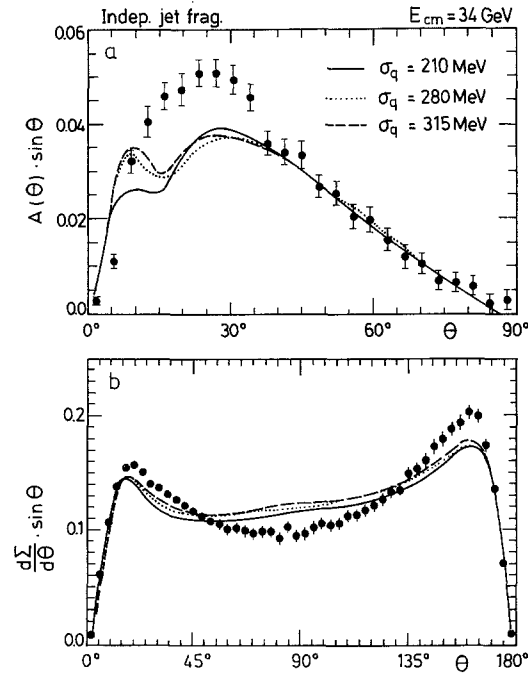


**Fig. 7a and b.** The asymmetry  $A(\theta)$  and the EEC  $d\Sigma/d\theta$  in comparison with the QCD calculations using the independent fragmentation model with  $A = 1.0$ ,  $B = 0.65$ ,  $y_{\min} = 0.0125$  and different values of  $\sigma_q$

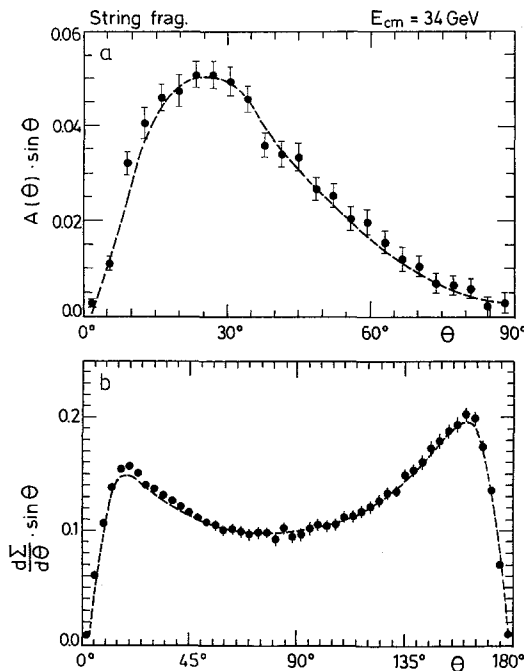


**Fig. 6a and b.** The asymmetry  $A(\theta)$  a) and the EEC  $d\Sigma/d\theta$  b) at  $E_{\text{cm}} = 34 \text{ GeV}$  compared with the QCD results using the string model fragmentation with following parameters:  $y_{\min} = 0.0125$ ,  $\sigma_q = 220 \text{ MeV}$ ,  $A = 1.0$ ,  $B = 0.70$  and  $\alpha_s = 0.165$ . The fit yields  $\chi^2_{\text{d.o.f.}} = 1.2(0.8)$  for  $d\Sigma/d\theta$  ( $A(\theta)$ )

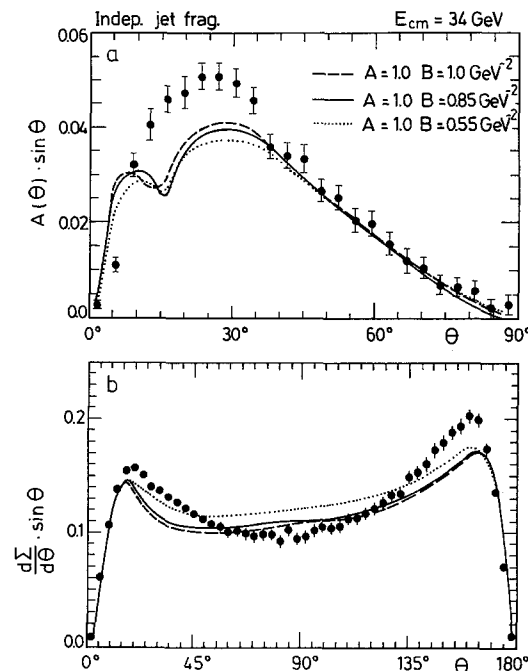


**Fig. 8a and b.** The asymmetry  $A(\theta)$  and the EEC  $d\Sigma/d\theta$  in comparison with the QCD calculations using the independent fragmentation model with  $\sigma_q = 240 \text{ MeV}$ ,  $y_{\min} = 0.0125$  and different values of  $A$  and  $B$

**Table 4.** The resulting best fit values of  $\alpha_s$  obtained by applying the different fragmentation schemes

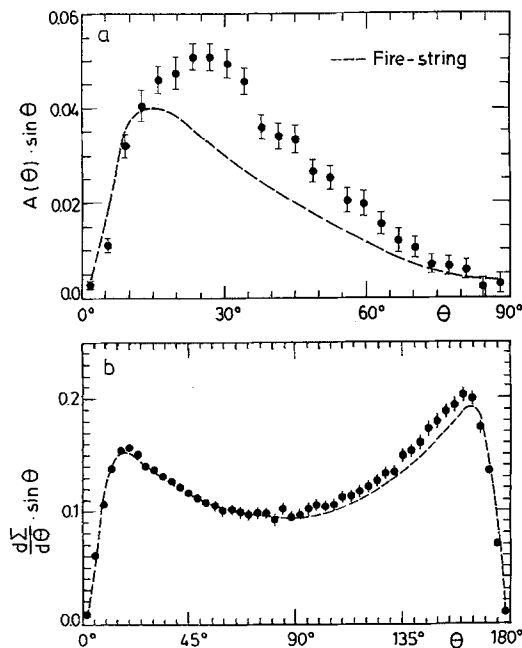
	(a) $g=q$	(b) $g \rightarrow q\bar{q}$ Altarelli Parisi	(c) $g \rightarrow q\bar{q}$ equally shared	String
(1) string				$\alpha_s = 0.165$
(2) indep. à la Hoyer	$\alpha_s = 0.112$	$\alpha_s = 0.115$	$\alpha_s = 0.105$	
(3) indep. à la Ali	$\alpha_s = 0.123$	$\alpha_s = 0.140$	$\alpha_s = 0.145$	

models. A reduction of  $Y_{\min}$  to 0.007 yields a somewhat better description of  $A(\theta)$  but increases on the other hand  $d\Sigma/d\theta$  around  $90^\circ$  beyond the already too high values shown in Figs. 7 and 8.

The resulting values of  $\alpha_s$  from the asymmetry in the region  $\theta > 36^\circ$  are given in Table 4 for the different model schemes. Note, that depending on the way energy momentum conservation is enforced and the gluon is treated,  $\alpha_s$  varies between 0.105 and 0.145. In all versions of the independent fragmentation schemes the EEC is badly reproduced yielding a  $\chi^2/\text{d.f.} > 10$  as evident from Figs. 7b and 8b.

### The Fire-String Model

As an example for an alternative to the perturbative QCD models we present a comparison with the fire-

**Fig. 9a and b.** The asymmetry  $A(\theta)$  and the EEC  $d\Sigma/d\theta$  in comparison with the prediction of the fire-string model

string model of Preparata et al. [19]. In the fire-string model, the two primary quarks are connected by a 'fire-string' which breaks up either into two subfire-strings or into a hadron and a rest string. The probabilities of the two decays are given by a matrix element. For more details see [19].

Figure 9 shows the comparison of this model with the data. In the region  $\theta < 90^\circ$  the EEC (Fig. 9b) is remarkably well reproduced, whereas for  $\theta > 90^\circ$  the curve is slightly below the data and the predicted asymmetry (Fig. 9a) fails to describe the data.

### Summary

Energy-energy-correlations between particles produced by  $e^+e^-$ -annihilation at  $E_{\text{CM}} = 14 \text{ GeV}$ ,  $22 \text{ GeV}$  and  $34 \text{ GeV}$  are presented in a form which allows for direct comparison with theoretical predictions. A comparison of the energy-energy-correlations and their asymmetries with various model calculations based on second order QCD shows that only the colour string fragmentation scheme reproduces the data quantitatively over the full angular range. It is interesting to note, that the study of an inclusive distribution like EEC confirms our earlier findings [20], which favour the string model from a detailed study of 3-jet events. The strong coupling strength in the  $\overline{\text{MS}}$  renormalisation scheme, deduced from this comparison, using the string model, is  $\alpha_s = 0.165 \pm 0.01$  (stat.)  $\pm 0.01$  (syst.) at  $\sqrt{s} = 34 \text{ GeV}$ . For the independent fragmentation models we obtained values of  $\alpha_s$ , ranging from 0.11, if momentum conservation is imposed according to Hoyer et al., to 0.15 if the scheme of Ali et al. is used. These values of  $\alpha_s$  are in good agreement with the value  $\alpha_s = 0.16 \pm 0.015$  (stat.)  $\pm 0.03$  (syst.) quoted previously [21] by our collaboration from a cluster analysis of 3-jet events covering both the Ali et al. and the Lund fragmentation scheme.

*Acknowledgement.* We acknowledge the efforts of the PETRA machine group, who provided us with the opportunity of doing this experiment, and also the efforts of the technical support groups of participating institutes in the construction and maintenance of our apparatus. We also thank T. Sjostrand for many useful discussions and suggestions. This experiment was supported by the Bundesministerium für Forschung und Technologie, by the Education Ministry of Japan, and by the U.K. Science and Engineering Research Council through the Rutherford Appleton Laboratory. The visiting groups at DESY wish to thank the DESY directorate for their hospitality.



## References

1. Y. Dokshitzer, D.I. D'yakonov, S.I. Troyan: Phys. Lett. **78B**, 290 (1978)
2. C. Basham, L. Brown, S. Ellis, S. Love: Phys. Rev. Lett. **41**, 1585 (1978); Phys. Rev. **D19**, 2018 (1979)
3. A. Ali, F. Barreiro: Phys. Lett. **118B**, 155 (1982); DESY 83-070 (1983)
4. D.G. Richards, W.J. Stirling, S.D. Ellis: Phys. Lett. **119B**, 193 (1982); Cambridge Univ. Report DAMTP 83/1 (1983)
5. S.D. Ellis: Phys. Lett. **117B**, 333 (1982)
6. PLUTO Collab., Ch. Berger et al.: Phys. Lett. **90B**, 312 (1980); **99B**, 292 (1981)
7. MARK II Collab., D. Schlatter et al.: Phys. Rev. Lett. **49**, 521 (1982)
8. CELLO Collab., H.J. Behrend et al.: Z. Phys. C – Particles and Fields **14**, 95 (1982); H.J. Behrend et al.: Phys. Lett. **138B**, 311 (1984)
9. MARK J Collab., B. Adeva et al.: Phys. Rev. Lett. **50**, 2051 (1983)
10. JADE Collab., W. Bartel et al.: Phys. Lett. **88B**, 171 (1979)
11. H.-J. Daum, H. Meyer, J. Buerger: Z. Phys. C – Particles and Fields **8**, 167 (1981); for cut parameters see: JADE Collab., W. Bartel et al.: Phys. Lett. **119B**, 239 (1982)
12. B. Andersson, G. Gustafson, G. Ingelman, T. Sjöstran: Phys. Rep. **97**, 33 (1983)
13. P. Hoyer et al.: Nucl. Phys. **B161**, 349 (1979)
14. A. Ali, E. Pietarinen, G. Kramer, J. Willrodt: Phys. Lett. **93B**, 155 (1980); A. Ali: Phys. Lett. **110B**, 67 (1982)
15. T. Sjöstrand: Comput. Phys. Commun. **27**, 243 (1982); *ibid.* **28**, 229 (1983)
16. K. Fabricius, G. Kramer, G. Schierholz, I. Schmitt: Z. Phys. C – Particles and Fields **11**, 315 (1982)
17. G. Altarelli, G. Parisi: Nucl. Phys. **B126**, 298 (1977)
18. B. Andersson, G. Gustafson, B. Söderberg: Z. Phys. **C20**, 317 (1983)
19. G. Preparata, G. Valenti: Nucl. Phys. **B283**, 53 (1981); B.L. Angelini et al.: Riv. Nuovo Cimento **3**, (1983)
20. JADE Collab., W. Bartel et al.: Z. Phys. C – Particles and Fields **21**, 37 (1983)
21. JADE Collab., W. Bartel et al.: Phys. Lett. **119B**, 239 (1982)